Optimal Traction Control for EV utilizing Fast Torque Response of Electric Motor

Xiaoxing Liu[1], Lianbing Li[1], Yoichi Hori[1],
[1]Department of Electrical Engineering
University of Tokyo
4-6-1 Komaba, Meguro
Tokyo153-8505, Japan
ryu@horilab.iis.u-tokyo.ac.jp
lilianbing@iis.u-tokyo.ac.jp
hori@iis.u-tokyo.ac.jp

Toru Akiba[2], Ryota Shirato[2]
[2]Technology Research Laboratory No.4, Nissan Research Center
Nissan Motor Co, Ltd
1 Natsushima-cho
Yokosuka 237-8523, JAPAN
t-akiba@mail.nissan.co.jp
r-shirato@mail.nissan.co.jp

Abstract— **It is well-known that the separately-wound DC motor has effective torque (current) reduction characteristics in response to rapid increase of the rotational speed of the motor. This characteristic has been utilized in adhesion control of electric locomotives with DC motor. In this paper, we have proposed a new slip prevention method for EVs, utilizing this characteristic and have made experiments with the hardware slip simulator "Motor-Generator setup" and our new vehicle "UOT CADWELL EV" which is equipped with BLDC motors. The experimental results verified the effectiveness of our proposed method.**

I. Introduction

In recent years, the Electric Vehicle (EV) has attracted considerable interests as one of hopeful solutions for solving environmental and energy problems. The advantages of EVs that comes up first are high efficiency and low pollution. The merits of the EVs, however, such as fast and precise output torque and so on have not been developed by present. The output torque of the motor can be controlled to follow its reference value accurately, with a relatively short time constant of 1[ms] and much less dead time. There are still many challenges and chances in the research of high-performance EV[1], [2], [3]. As an excellent example making use of fast response of EVs, the separately-wound DC motor with the torque (current) reduction characteristics is researched in this paper to develop a new slip prevention method between the EV and the road [4].

II. Slip prevention control based on torque reduction characteristics of separately-wound DC motor

A. Vehicle Dynamic Model

Suppose that the time constant, the rolling resistance and the wind drag force are very small. The forces effecting on the vehicle are shown in Fig.1, and the dynamic equations are expressed in Equation (1) - (3).

$$\omega = \frac{1}{Js}(T - rF_d) \quad (1)$$

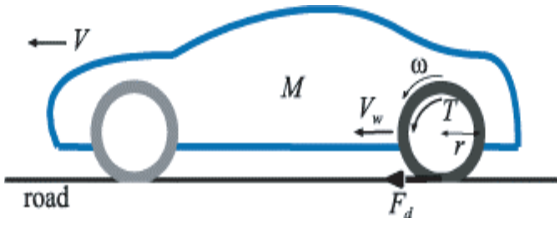

Fig. 1. Motion of vehicle

$$V = \frac{1}{Ms}F_d \quad (2)$$

$$V_w = r\omega \quad (3)$$

Where ω is the rotational speed of the wheel (motor), V is the speed of the vehicle, V_ω is the speed of the wheel, F_d is the driving force, T is the driving torque of the motor and s is the Laplace operator. J is the inertia moment of all the rotating parts of the EV, r is the radius of the tire and M is the mass of the EV.

Equation (1) is the motion equation of the wheel, and the wheel is effected by the torque of the motor and the reaction force from the road. Equation (3) is the motion equation of the chassis.

B. Adhesion Characteristics of Tire and Road

The adhesion characteristics of tire and road can be expressed by the concept of slip ratio. Slip ratio λ is defined in the following equations utilizing V, V_w,

$$\lambda = \frac{V_w - V}{V_w}(Driving) \quad (4)$$

$$\lambda = -\frac{V - V_w}{V}(Braking) \quad (5)$$

Utilizing slip ratio λ, the relationship of the slip ratio and the friction coefficient μ between the tire and the road can be approximated and described, for example, by Equation (6), which is called $\mu - \lambda$ curve (function).

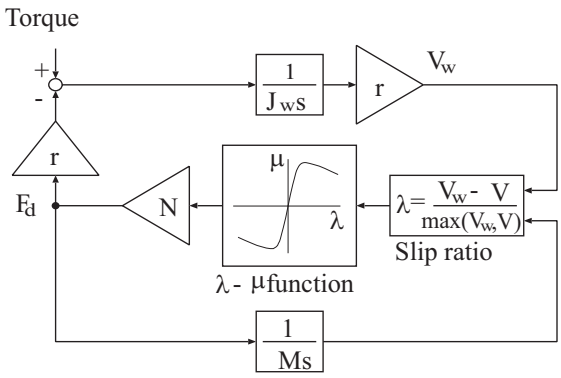

Fig. 2. Block diagram of the one-wheel vehicle model

$$\mu = -1.05k\exp(-45\lambda) - \exp(-0.45\lambda)(Driving) \quad (6)$$
$$\mu = 1.1k\exp(35\lambda) - \exp(0.35\lambda)(Braking) \quad (7)$$

Where k is the parameter of the road status, and takes the following values, for example,

$$k = 1(Dryroad) \quad (8)$$
$$k = 0.2(Icyroad) \quad (9)$$

After having achieved the friction coefficient μ from slip ratio λ utilizing $\mu - \lambda$ curve, the driving force F_d can be calculated by Equation (10).

$$F_d = \mu(\lambda)N \quad (10)$$

Where N is the normal component of reaction effecting on tires. The model of the one-wheel EV can be shown in Fig.2.

C. The Slip Prevention Scheme utilizing Back-EMF

The block diagram of the EV system installed separately-wound DC motor is shown in Fig.3. G^{-1} in Fig.3 is the inverse function of the transfer function from the voltage command v^* to the current i. It is utilized to acquire the voltage command v^*.

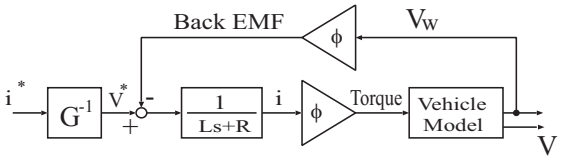

Fig. 3. Block diagram of the EV system installed separately wound DC motor with FF current control

Suppose that the vehicle is running from the dry road to the icy road, and the surface of the icy road is very smooth, so that the friction between the tire and the road is rapidly reduced. At the same time the motor of the EV is still keeping the driving torque as before, then the wheel will slip on the icy road quickly.

If the torque (current) reduction characteristics of the separately-wound DC motor, however, can be activated, the slip phenomenon will be restrained. Though the speed of the wheel quickly increases, the back-EMF that is proportional with the rotational speed of the wheel will increase at the same time to decrease the acceleration of the wheel. This is the scheme of the slip prevention utilizing torque (current) reduction characteristics of separately wound DC motor.

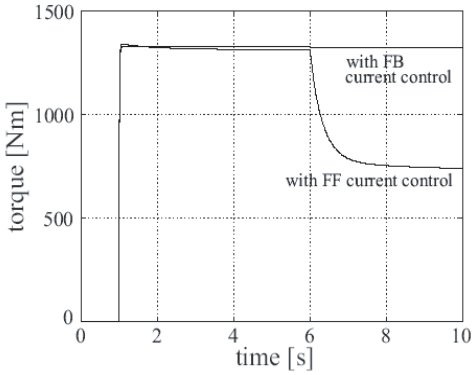

Fig. 4. Torque

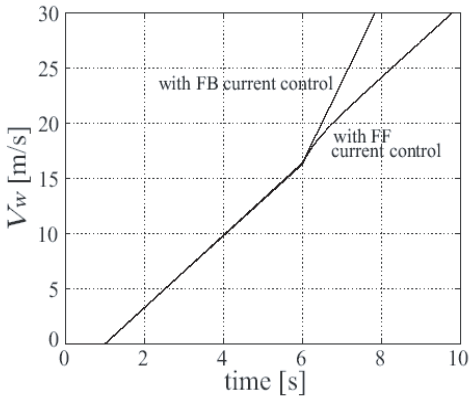

Fig. 5. Wheel speed

The advantage of this method is that the complicated calculation is not necessary and the torque (current) can be decreased quickly.

Slip phenomenon is simulated utilizing the EV system as shown in Figs.2 and 3. The simulation is started at $t = 0[s]$. At $t = 1[s]$, the EV starts to accelerate in the dry road, and at $t = 6[s]$ it enters the icy road. The parameters of the EV system are utilized by "UOT March I" which is the experimental EV of our laboratory.

The simulation results are shown in Fig.4-7. For the sake of comparison, the curves controlled by FB current controller and by FF controller are shown in the same figures. The curve with FF current control in Fig.4 shows the torque reduction characteristics. As a result, the slip is restrained as shown in Figs.5 - 7[5].

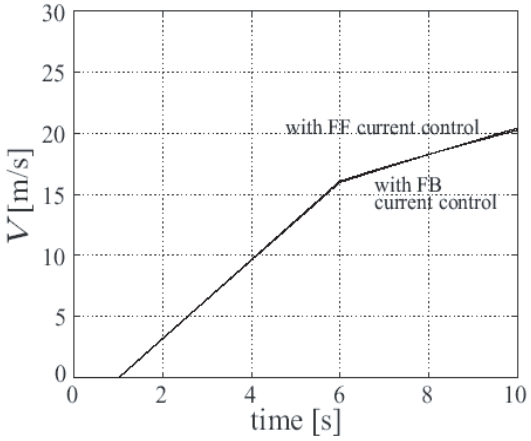

Fig. 6. Vehicle speed

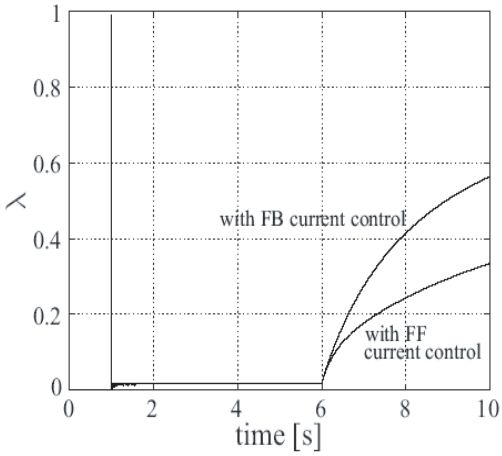

Fig. 7. Slip ratio

D. Experimentation of Motor-Generator Setup

D.1 Outline of Experimentations

Motor-Generator setup is shown in Fig.8 and the sketch of control system is shown in Fig.9. The torque (current) reduction when the vehicle slips and the circumstances that the disturbance observer adjusts torque reduction characteristics is observed utilizing Motor-Generator setup, where the shafts of two motors (the driving motor and the loading motor), are interconnected. The loading motor is controlled by the only hardware control-boards and the inertia moment of the loading motor seen from the driving motor can be controlled. The driving motor is controlled by the hardware control-boards and software one. That is to say, PI controller, driver of the motor and so on consist of hardware, but disturbance observer and G^{-1} filter are designed as software controller. DA, AD, counter boards act as a bridge between hardware and software. The sampling time of the software controller is $1[ms]$. The current command $i^* = 2[A]$, the inertia moment is rapidly decreases at about $t = 3[s]$, which means the vehicle begins to slip.

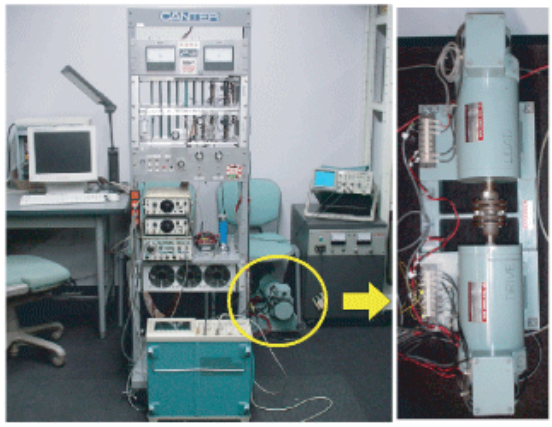

Fig. 8. Motor-Generator setup system

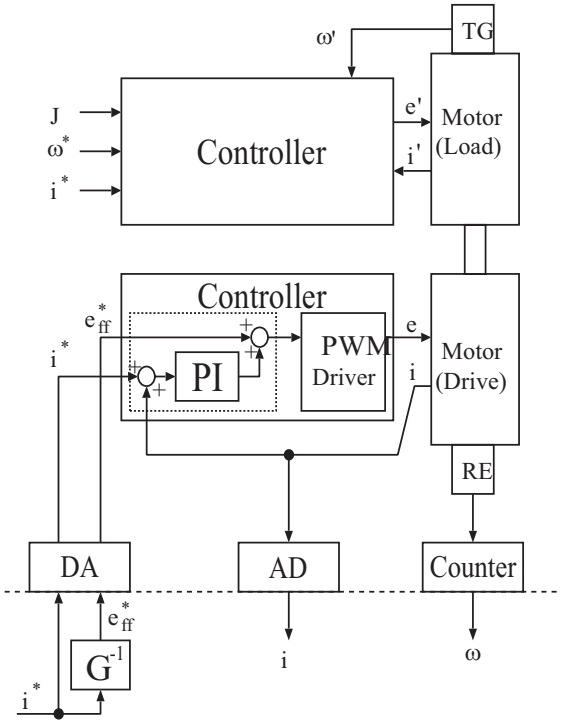

Fig. 9. Block diagram of the sontrol system utilizing Motor-Generator setup (The PI controller is not utilized)

D.2 Confirmation of Torque (Current) Reduction Characteristics

The experimental test was performed in order to confirm the torque (current) reduction characteristics shown in previous section. The current of the motor and the rotational speed are observed at the accelerated speed when the vehicle slips both in the case that pre-filter G^{-1} shown in Fig.3 is only added to separately-wound DC motor and in the case that the motor is controlled only by the current controller. Results are shown in Fig.10 and 11.

The inertia moment of the motor which is simulated the slip phenomenon decreases rapidly at about $t = 3[s]$. Fig.10 shows that the current of the motor reduces when the inertia moment decreases if only pre-filter is being utilized. Therefore, the rotational speed of the motor is pre-

vented from rapid increase in Fig.11. In contrast, the rotational speed of the motor is, as a result, rapidly increased since the current of the motor is held constant when utilizing the FB current controller even if the inertia moment decreases.

In conclusion, it proved that the proposed slip prevention method utilizing torque(current) reduction characteristic prevents vehicle equipped with separately-wound DC motor form skidding effectively.

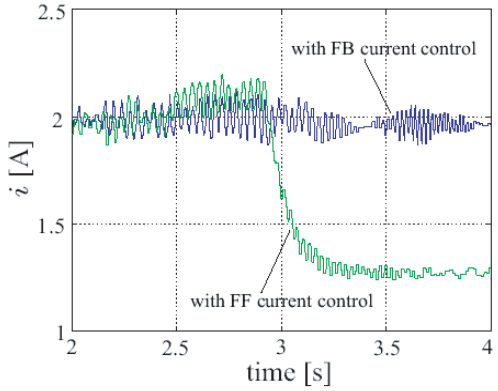

Fig. 10. Current of the motor reduces only when it is controlled with FF current controller

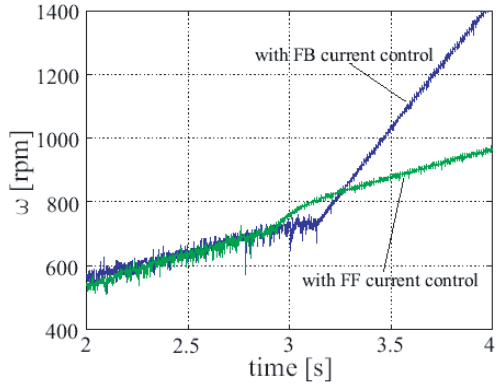

Fig. 11. Rotational speed of the motor is prevented from rapid increase only when it is controlled with FF current controller

III. Practical Experiments of Vehicle "UOT CADWELL EV" Equipped with BLDC Motors

Up to now, we have proposed a new slip prevention method for EVs, utilizing this characteristic and have made experiments with the hardware slip simulator "Motor-Generator setup". From this chapter, an implement method for applying this slip prevention control to our new vehicle "UOT CADWELL EV" equipped with BLDC motors is proposed and demonstrated. The experimental results of "UOT CADWELL EV" verified the effectiveness of our proposed method.

A. Vector control of BLDC motor

Necessary various variables and various constants used in vector control of BLDC motor are shown in Table 1.

TABLE I
Parameters and constants.

V_d	d-axis armature-votage	R_a	armature resistance
V_q	q-axis armature-votage	L_d	d-axis inductance
i_d	d-axis armature-votage	L_q	q-axis inductance
i_q	q-axis armature-votage	ϕ_a	magnetic flux
ω_{re}	electrical angular velocity	T	torque
ω_{rm}	mechanical angular velocity	J	moment of inertia
θ_{re}	electrical angular	P	d/dt

The equivalent circuit of BLDC motor is expressed in (11)

$$\begin{bmatrix} v_d \\ v_q \end{bmatrix} = \begin{bmatrix} R_a + pL_d & -\omega_{re}L_q \\ \omega_{re}L_dR_a & +pL_q \end{bmatrix} \begin{bmatrix} i_d \\ i_q \end{bmatrix} + \begin{bmatrix} 0 \\ \omega_{re}\psi_a \end{bmatrix} \tag{11}$$

In order to realize the slipping control by the FF current control proposed in previous chapter, two filters (Filter1,Filter2) are added composing the usual vector control of BLDC motor. Figure.12 shows the vector control configuration of the EV system equipped with BLDC motor which is contained both the usual FB current control and the proposed FF control (Equation 16).

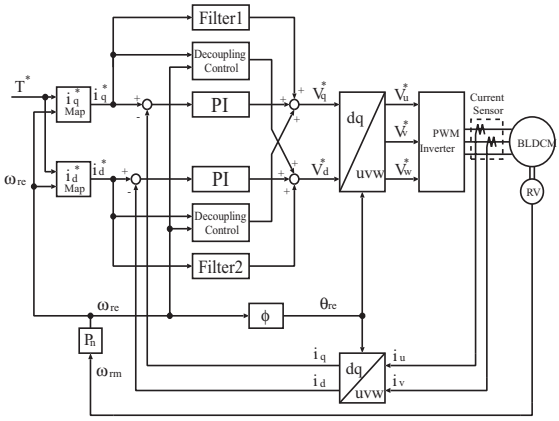

Fig. 12. Vector control configuration of the EV system equipped with BLDC motor

B. FF+FB current control

Figure.13 shows the block diagram of the EV system equipped with decoupling controlled BLDC Motor. From this figure, $G_q(s)$ the transfer function from v_q^* to i_q and $G_d(s)$ the transfer function from v_d^* to i_d are obtained by

$$\begin{aligned} G_q(s) &= \frac{i_q}{v_q^*} \\ &= \frac{1}{L_q s + R_a + \frac{P_n^2 \psi_a^2}{Js}} \end{aligned}$$

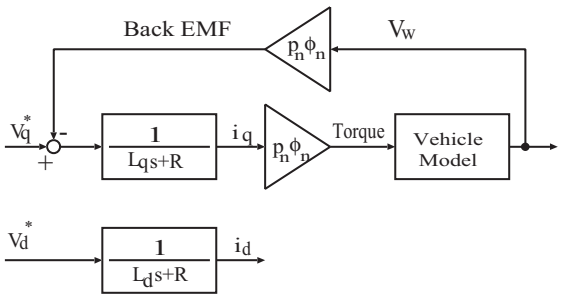

Fig. 13. Block diagram of the EV system equipped with decoupling controlled BLDC Motor

$$\begin{aligned} &\simeq \frac{J}{P_n^2\psi_a^2}\frac{s}{(1+\tau_e s)(1+\tau_m s)} \\ &\simeq \frac{J}{P_n^2\psi_a^2}\frac{s}{1+\tau_m s} \\ G_d(s) &= \frac{i_d}{v_d^*} \\ &= \frac{1}{L_d s + R_a} \end{aligned} \tag{12}$$

Where mechanical time constant τ_m and electrical time constant τ_e are expressed in (13),(14).

$$\tau_m = \frac{JR_a}{P_n^2\psi_a^2} \tag{13}$$

$$\tau_e = \frac{L_q}{R_a} \tag{14}$$

Because there is only q axis torque element that takes part in the calculation of vector control, inverse function $G_q^{-1}(s)$ of $G_q(s)$ is shown in Equation (15)

$$\begin{aligned} G_q^{-1} &= \frac{P_n^2\psi_a^2}{J}\frac{1+\tau_m s}{s} \\ &= \frac{P_n^2\psi_a^2}{J}\frac{1}{s} + R_a \end{aligned} \tag{15}$$

Therefore, filter F is defined by

$$\begin{aligned} F &= \begin{bmatrix} Filter1 \\ Filter2 \end{bmatrix} \\ &= \begin{bmatrix} G_q^{-1}(s) \\ 0 \end{bmatrix} \end{aligned} \tag{16}$$

In this system, slipping is restrained by using the FF filter for q axis utilizing torque (current) reduction characteristic in the micro time scale when slipping occurs. Though in macro time scale, the FB current control is used to output the provided torque. That is, it becomes a hybrid current control with the FF filter and FB current control whose proportional gain has been reduced from optimal value. D axis that doesn't take part in calculating the torque only use a conventional FB current control.

C. Experimentation of "UOT CADWELL EV"

C.1 configuration of "UOT CADWELL EV"

"UOT CADWELL EV" is shown in Figure.14. It has two BLDC motors that can be driven independently. The proposed hybrid current control has been realized by MIC (Motor Inverter Controller) instead of vehicle control PC. Interface box matches various electric characteristics (various sensor information, communication between MIC and control PC) to vehicle control PC.

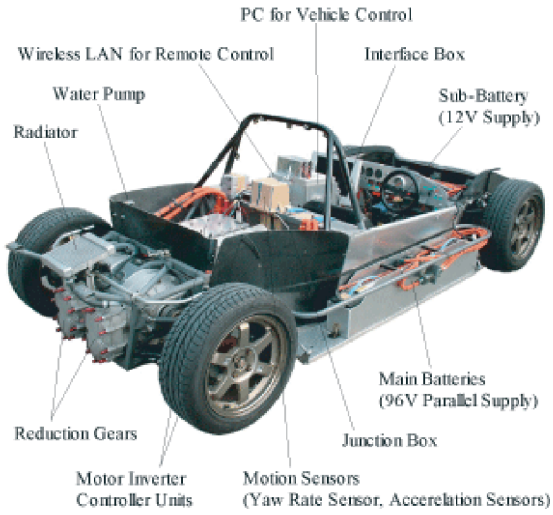

Fig. 14. Configuration of "UOT CADWELL EV"

C.2 Experimental results

The experiment results when vechile were driven from dry road into slippery road utilizing usual FF current control and proposed FF+FB current control are shown in Figure.16 and Figure.17.

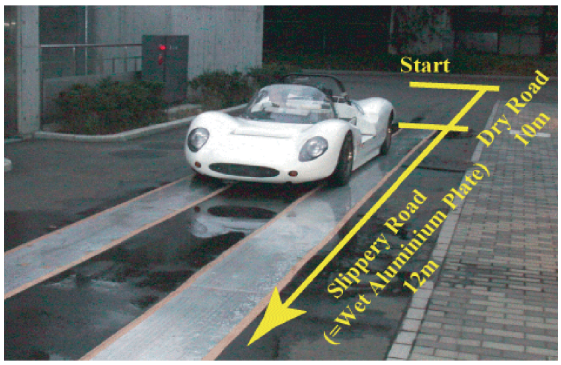

Fig. 15. Appearance of the Experiment

Figure.15 shows the appearance of this experiment. Because re-adhesion instantly occurs when FF filter based on torque (current) reduction characteristic activates. The current of the motor does not reduce as the results acquired by Motor-Generator setup system. As a result, obviously utilizing only FB current control, the rotational speed of the motor rapidly increases when the slip occurs. But the

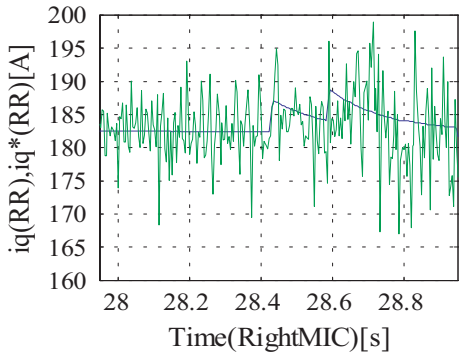

(a) Current of the motor

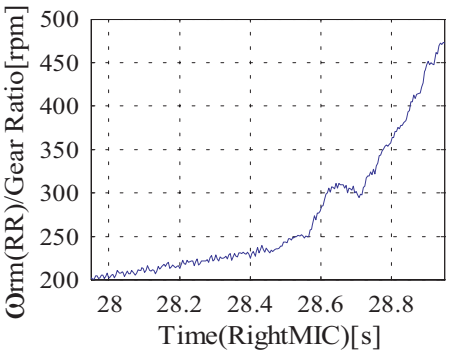

(b) Rotational speed of the motor

Fig. 16. Experimental results of the slip phenomenon with FB current control

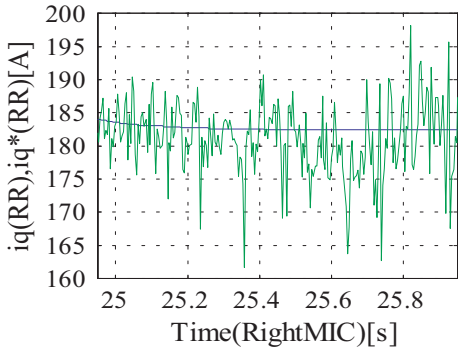

(a) Current of the motor

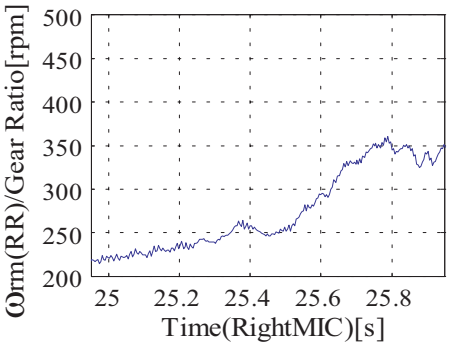

(b) Rotational speed of the motor

Fig. 17. Experimental results of the slip phenomenon with FF+FB current control

speed of the motor is prevented from rapidly increasing when proposed FF+FB current control is used.

IV. Conclusion

The AC motor made of permanent magnet is the most appreciated and most commonly utilized for EVs at the present day and it is controlled by the high-performancecurrent controller. However because of its poor adhesion performance, this current control is shown necessary to be improved though our research.

In this paper, it proposed the traction control for EV utilizing fast torque response of electric motor. Its effectiveness has been confirmed by the experimental results using Motor-Generator setup and "UOT CADWELL EV".

If the development of our studies comes to be utilized widely, needless to say, the risk of slip becomes dramatically small. It also can contribute greatly to safety improvement of the vehicle utilizing the advanced attitude control system even if driving on the skiddy road.

References

[1] Y. Hori, "Traction Control of Electric Vehicle: Basic Experimental Results Using the Test EV UOT Electric March," IEEE Trans. on Industry Applications, Vol. 34, No. 5, pp.1131-1138, 1998.

[2] S. Sakai and Y. Hori, "Advantage of Electric Motor for Anti Slip Control of Electric Vehicle," EPE Journal, Vol.11, No.4, pp.26-32, 2001.

[3] S. Matsugaura, et al., "Evaluation of Performances for the In-Wheel Drive System for the New Concept Electric Vehicle KAZ," in Proc. EVS19, Pusan, Korea, 2002.

[4] T. Miyamoto and Y. Hori, "Adhesion Control of EV Based on Disturbance Observer," IEE of Japan Technical Meeting Record, IIC-00-9, pp.49-54, 2000. [In Japanese]

[5] S. Kodama, L. Li and Y. Hori, "Skid Prevention for EVs based on the Emulation of Torque Characteristics of Separately-wound DC Motor," in Proc. AMC-2004, 2004.3.25-27, Kawasaki